DOI: 10.4408/IJEGE.2011-03.B-039

MODELLING DEBRIS FLOW PROCESSES WITH A GEOTECHNICAL CENTRIFUGE

P. KAILEY(*), E.T. BOWMAN(*), J. LAUE(**) & S.M. SPRINGMAN(**)

(*) University of Canterbury, Christchurch, New Zealand
(**) Institute for Geotechnical Engineering, ETH Zurich, Switzerland (*) Affiliation

ABSTRACT

In this paper, we examine the effect of flow mass and moisture content on debris flow velocity, discharge, and runout using a series of smallscale flume tests in a geotechnical centrifuge. We found that an increase in mass and an increase in moisture content increased peak velocity during down-slope movement. However, the effect of increased moisture content is much more pronounced than that of increased mass. The maximum cross-sectional area observed did not depend on mass or moisture content, although may have been affected by the flow rate entering the centrifuge. Consequently, flow velocity largely determined the peak discharge of each flow. An increase in moisture content increased the mobility of the flow in terms of depositional area and runout. Further, the runout of the centre of mass of the flows appears to be linearly related to the momentum of flow material entering the flume.

Key words: *debris flows, physical modelling, runout, velocity, centrifuge tests*

INTRODUCTION

PHYSICAL MODELLING OF DEBRIS FLOWS

The highly complex, stochastic nature of debris flows is a direct result of the synergistic interaction between their fluid and solid phases. Key debris flow parameters such as particle size distribution, moisture content, velocity, and discharge vary spatially and temporally as a debris flow travels down its path, which complicates understanding and modelling the mechanics of debris flow motion. Even if one is lucky (or unlucky) enough to be able to observe a debris flow event in the field, the boundary conditions and key parameters influencing flow behaviour may be difficult or even impossible to measure.

Physical modelling simplifies these processes and allows boundary conditions to be controlled in the laboratory, without preconditioning the outcome. This has made small-scale flume studies of debris flows an indispensible tool in elucidating some key aspects of debris flow mechanics. However, there are some drawbacks to flume studies at the small scale. The extrapolation of small-scale behaviour to field scale processes may not always be appropriate, as small scale flows may not reflect the dominance of Coulomb stresses and decreasing importance of viscous stresses in field scale flows (Denlinger & Iverson, 2001). In previous work, Bowman *et alii* (2010) showed that the centrifuge can match particular aspects of large-scale behaviour well, which would be difficult at the small scale at 1-g. In particular, the centrifuge tests reproduced low Savage and Pore Pressure numbers, ensuring that centrifuge flows are in the frictional regime and can maintain persistently high pore-pressures, like large scale flows. The other principle advantage of centrifuge testing is that they can potentially be more convenient and flexible than large scale experiments, as flume geometry can be altered. They also require

less material than large scale flume tests.

The aim of the experiments presented in this paper was to extend the work of Bowman *et alii* (2010) by investigating theinfluence of flow mass and mois ture content on debris flow behaviour in the centrifuge, as these parameters are considered key to the development of debris flow velocity, discharge, and runout. It also addresses some experimental difficulties and recommendations for improvement in future centrifuge studies.

It should be noted that, coming from a geotechnical perspective, we use moisture content by mass, rather than solids concentration by volume as often used elsewhere in the debris flow literature. The relationship between them is:

$$C_v = \frac{1}{G_s w + 1}$$

Where C_v is the solid concentration by volume, w is the moisture content by mass and Gs is the specific gravity of solids, taken here to be 2.65. A moisture content of 33% or 0.33 corresponds to a solids concentration of 0.53 by volume.

Debris flow volume is often cited as the most critical parameter in estimating debris flow hazard, as larger flows travel faster and farther than smaller flows, both at the laboratory and field scale. This is likely due to be due to the prevalence of high pore pressures which are more likely to be maintained in a thicker flow due to longer drainage paths (Bowman *et alii*, 2010). Previous work has shown that the peak discharge of the flow can be related to the debris flow volume (Rickenmann, 1999).

Test Code	Mass of solid material used (kg)	Moisture content (by mass)
T14	1.5	33%
T15	1.0	33%
T20	2.5	33%
T23	1.75	39%
T11	1.75	41% (+/- 1%)

Tab. 1 - Test code and short description of each test. All tests were conducted over a fixed bed, using a mixture of glycerine and water as a viscous pore fluid (μ=42cP, or 42 time the viscosity water at 20°C). Moisture content was calculated by (mass of pore fluid/mass of solid)× 100

Moisture content within the flow can be just as important as event volume. For example, in field investigations in the Dolomites and small-scale flume investigations, moisture content appeared to control runout, almost regardless of event volume (D'Agostino *et alii*, 2010). Takahashi (2007) also discusses the importance of moisture content in controlling the velocity distribution of particles with depth.

Preliminary results from five debris flow tests are presented. Three tests were run using different masses of solid material (1, 1.75, and 2.5kg) with a uniform moisture content (by mass) of 33%. Two final tests were run using 1.75kg of material, with moisture contents of 39% and approximately 41%, respectively.

The purpose of these last tests was to investigate the influence of moisture content (Table 1). The moisture content in T11 is only approximate. The first attempt at T11 became clogged in the feeder tube. Since centrifuge time, and time to prepare the material, was limited, the test was rerun by adding the approximate volume of fluid lost in the first attempt. While the range of moisture content tests varies by only 8%, the effect on flow behaviour, as discussed below, is dramatic. This range of moisture content was also convenient to test, as at moisture contents below 33%, the flow consolidates very quickly. Above 41%, it became more difficult to manage as more material was lost during the transition from the feeder tube to the head of the flume, as well as during collection.

CENTRIFUGE TESTING

APPARATUS AND INSTRUMENTATION

Details regarding the design and instrumentation used in the experiments have been discussed previously (Bowman *et alii*, 2010). However, a brief description of the apparatus and some minor changes to the flume, relevant to the following discussion, is given below.

Experiments were carried out using the ETH Zurich Geotechnical Drum Centrifuge in Switzerland (Springman *et alii*, 2001). This centrifuge has a maximum working radius of 1.1m, a maximum design acceleration of 440g and a maximum load carrying capacity of 2000kg.

The debris flow apparatus was designed to guide liquefied debris flow material from its head to the inner circumference of the centrifuge drum. The drum circumference itself was used as the runout zone – i.e. where the flow comes to rest. Several holes located

along the circumference of the drum allowed fluid to drain from the consolidating debris flow.

The debris flow flume apparatus consisted of a channel, a strut and a curved support to spread load to the drum. The 700mm long flume followed the inner curvature of the drum, such that, at a slope angle of 0°, it would lie evenly along the drum circumference. The flume width in this round of tests was decreased from 160mm, as used in previous tests, to 60mm to provide increased channelisation, and hence increased flow depth, and velocity towards values more representative of field scale flows than those obtained previously. The confinement ratio (flow height/width of channel) observed in these tests was approximately 4. Previous field studies in coarsegrained debris flows have found the onset of deposition to occur at confinement ratios of 5 to 7 (Hungr *et alii*, 1984; King, 1996). The increased flow depth combined with a coarser particle distribution enabled individual particles to be tracked in the high speed camera images, as discussed later.

Six pore pressure transducers (PPTs) were provided along the base of the flume for the measurement of pore pressure during the experimental debris flows. Coarse sand particles glued to the base provided a rough substrate; the smooth aluminium and Perspex walls ensured relatively plane strain behaviour.

A small monochrome high-speed digital camera (operating at 330 frames per second) was used to observe the flow through the clear, Perspex channel wall. Small markers were painted on the window to provide scale and reference points to track the flow. The flow was lit by a close array of 8 LEDs embedded in the Perspex window.

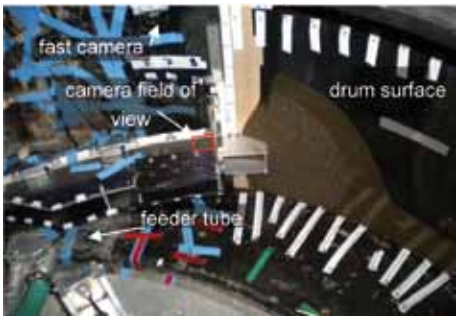

Fig. 1 - Photograph of experimental set-up and deposition from test T14, which has consolidated on the drum surface after spin-down. The markers in the top of the photograph serve as reference points for point measurements of depth. Note that the photo was taken obliquely, the deposition is plastered vertically to the inner wall of the drum

Unconsolidated debris flow material was introduced "in flight" to the channel by a flexible tube. The tube extended from the central axis of the centrifuge, where material was delivered via a funnel, and was guided by an actuator on the centrifuge tool plate to the head of the channel, where it exited to flow outward under centrifugal acceleration, down the slope. This system enabled the material to be prepared and maintained as a slurry external to the drum (in which it would otherwise consolidate during spin-up).

After each test, measurements were taken of the maximum runout and lateral spread of each flow. In addition, markers running vertically and horizontally on the drum surface were used as a grid to record spot depths of the flow deposition (Figure 1). These data were then used to compare the morphology of deposition and runout.

CENTRIFUGE SCALING PRINCIPLES

Scaling relationships for geotechnical centrifuge modelling are shown in Table 2 (Steedman & Zeng, 1995). Note that inertial effects (which scale to 1/N) and diffusional effects (which scale to 1/N2) scale differently over the same time period. To resolve this inconsistency, the prototype pore fluid (assumed to be water) is replaced with a higher viscosity pore fluid, which inhibits consolidation, allowing pore pressures to develop as at prototype scale. A glycerine and water mixture with viscosity of the pore fluid of approximately N times higher than water (1cP) is usually chosen. This reduces the time for consolidation by N2 and inertia by N in the model, resulting in the same over-

Parameter	Prototype (field)	Model (centrifuge)
Gravity acceleration	g	Ng
Stress	σ	σ
Displacement	x	x/N
Velocity	V	V
Acceleration	a	aN
Time (inertial)	t_i	t_i/N
Frequency	F	F
Time (diffusional)	t_d	t_d/N^2
Energy	E	E/N^3

Tab. 2 - Scaling laws used in geotechnical centrifuge testing, based on $N\times g = r\times\omega 2$, where ω is angular velocity (STEEDMAN & ZENG, 1995). N is the g-level, hence at a gravitation acceleration of 40g, N=40

all time for these processes as in the prototype with water. This approach also means that the particle size distribution (PSD) used in the experiments is the same as the PSD at the prototype scale in terms of consolidation behavior. In these experiments, all tests were run at 40g with a 42cP pore fluid, due to the difficulty of achieving an exactly 40cP solution. This resulted in the prototype and model PSD shown in Figure 2.

The mass of solid material used in these tests was varied from 1 kg to 2.5 kg, which corresponds to 40 kg to 100 kg at the prototype scale. The prototype channel dimensions scale to 28 m long by 2.4 m wide. Peak flow heights were recorded between 14 and 17 mm high, corresponding to a prototype flow height of 0.56 to 0.68 m.

While the prototype length scales and PSD come close to replicating some small, field-scale debris flows, this prototype was not chosen to replicate any particular event and should still be considered highly idealised.

MATERIAL CONSTRAINTS

The material used in these tests was a mixture of soil from three separate localities, two in New Zealand and one in Switzerland. The largest fraction used (approximately 48% by weight) was collected from the Mt. Thomas debris flow site in Northern Canterbury. This locality has been a site of ongoing debris flow activity since 1977, when a series of debris flows were triggered on recently harvested cut blocks (Pierson, 1980). The material from Mt. Thomas was supplemented in the range of 0.6mm to 0.075mm with Swiss fluvial material, since there was relatively little fine sand and silt available from the Mt. Thomas material. 41% of the PSD tested was made from the fluvial material. The lighter colour of this sand also created more texture in the high speed camera images, which was useful for post-processing. The remaining 11% of the mixture came from nonplastic loess collected from slips in the central north island of New Zealand. This provided the remainder of the, silt and minor clay in the particle size distribution used in the tests (Figure 2). All material was carefully sieved, then mixed to the desired particle size distribution before each test.

Experimental constraints limit the particle size distribution tested in the centrifuge. The maximum size particle used is limited by the internal diameter in the feeder tube In this case, the internal diameter of the feeder tube was 32mm and the maximum particle diameter was approximately 8mm. Particles larger than this cause chronic mechanical arching and flow blockage. Even with the PSD used, we did have a test which clogged (test 11, as discussed previously). The particle size distribution tested represents a compromise between the largest possible particle size, represented by d_{90} (the particle size at which 90% of particles by mass are smaller than) of 2mm, while still allowing a relatively high value of Cu (d_{60}/d_{10}) of 36.7, which is shown to be an important parameter in other physical modelling studies of debris flow behaviour (Bowman & Sanvitale, 2009).

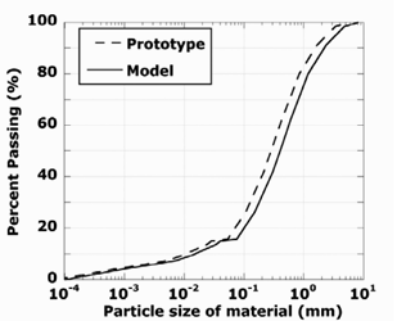

Fig. 2 - Model (actual) and prototype PSD used in all tests. All tests were run at 40g with a 42cP pore fluid, shifting the prototype PSD slightly to the left

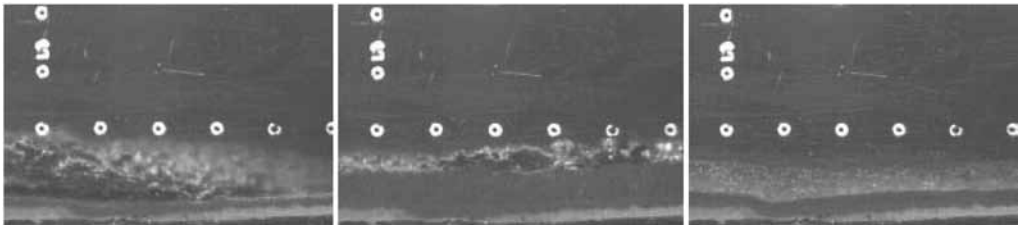

Fig. 3 - High speed camera images from T14, frames (a) 644, (b) 707, (c) 1501. Flow proceeds from left to right. The dot spacing is 10 mm. The sequence shows (a) the arrival of the front, (b) thickening of the front, and (c) transition to the watery tail portion of the flow

TEST RESULTS

HIGH SPEED CAMERA IMAGES AND FLOW HEIGHTS

Images from the high speed camera gave a view of the debris flow as it passed the Perspex window. A fast, coarse, unconfined flow front dominated by larger diameter solids preceded the peak discharge in every flow (Fig. 3).

The surface of each flow was nearly always slightly higher in the middle than on the edges because larger particles were often carried in the center of the flow and their edges would protrude from the surface. While particles adjacent to the Perspex window were in focus, particles near the centre were somewhat blurry and indistin because of the limited depth of field in the camera. This can be seen quite clearly in Figure 3. To explore the change in flow depth over time, the flow heights, both at the free surface at the center and against the window, were measured by use of the high speed camera images. Measurements were taken at least every four frames during front passage, then every several hundred frames in the watery tail portion of the flow when the rate of change of flow height dropped significantly. These measurements were precise to within ±0.5mm. A cross-sectional area for each frame was calculated from these data.

The depth of flow rapidly attenuated in all the flows, and then slowly decreased in accordance with a near-power law (Fig. 4). The transition to the tail portion of the power-law plot roughly coincided with an apparent sudden increase in moisture content (visible as a change in texture of the soil against the window and reduction in flow surface roughness), reflecting the transition to the "watery tail" portion of the flow.

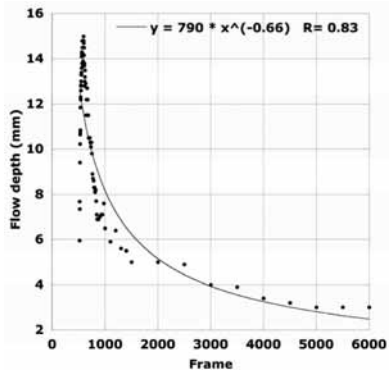

Fig. 4 - Change in flow depth with time for test T15.

Observations from the high speed camera also enabled the surface velocity of the flow over time to be determined. By tracking individual particles over several frames (as many frames as each particle was distinguishable), an instantaneous velocity of the particle could be determined. These velocity data were` used to construct the debris flow hydrographs and velocity profiles discussed later in the paper.

FLOW VELOCITY

Pore pressure transducers mounted in the flume and high speed camera data were used to reconstruct the velocity of the flows as they travelled down the flume (Fig. 5). The locations of the data points shown in Figure 5 are half way between the PPTs, which recorded the responses used to calculate the velocity. Figure 5 also shows velocity recorded by the high speed camera near the flume outlet. This camera velocity was calculated by tracking how long it took the flow to traverse the width of the camera frame (approximately 100mm). Mixing data-points calculated from porepressure data with visual data is not ideal, as the pore pressure data could have a small lag in response time, especially as the PPTs may not register an unsaturated, 'bouldery' front. The provision of an additional, wider angle camera recording the flow from above, or additional PPTs near the channel bottom would solve this issue.

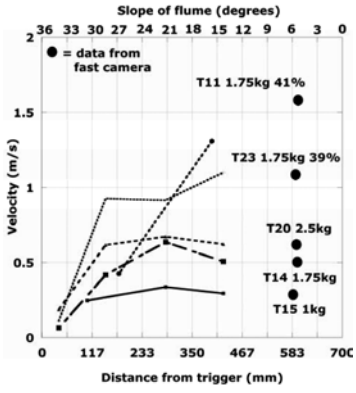

Fig. 5 - Debris flow front velocity versus distance down slope from light switch. T14, T15 and T20 have varying masses of material at 33% moisture content, whereas T23 and T21 have a mass of 1.75kg and greater moisture contents. The slope of the flume is shown on the secondary x-axis. The moisture content of T11(41%) is accurate to within ±1%, as discussed in the text

Both debris flow volume and moisture content significantly affected flow velocity. The tests conducted with 33% moisture content all show the same general trend; flow velocity increases to a point nearly half-way down the flume, then begins to decelerate. As expected, an increase in mass causes the velocity to increase. An increase in moisture content, however, has a much more profound effect on velocity than mass. Comparing T11 (1.75 kg at approximately 41%), and T14 (1.75 kg at 33%), an increase of 8% in moisture content increased the peak velocity by a factor of 3.

All three flows at 33% moisture content began to slow at a slope angle of approximately 21º (Figure 5), while the flows at higher moisture contents show deceleration at around 15º.

These angles coincide with the range of slope angles shown to be transitional between entrainment, transport, and deposition in the field (Fannin & Wise 2001). In the Queen Charlotte Islands, Fannin & Wise (2001) found that for coarse-grained, channelized flows in unconfined reaches, slope angles between 19º and 24º were found to have both deposition and entrainment. In confined reaches, both deposition and entrainment occurred on slope angles between 10º to 22º Deposition was the dominate process for confined reaches at slope angles of less than 10º.

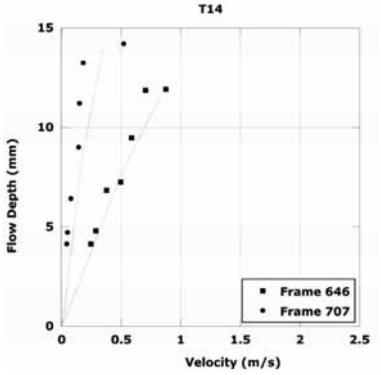

Fig. 6 - Velocity profile with depth for T14 (1.75kg, 33% moisture content). Frame 646 records the flow front, while frame 707 captures the velocity m profile in the falling limb of the flow hydrograph, just after the peak flow height

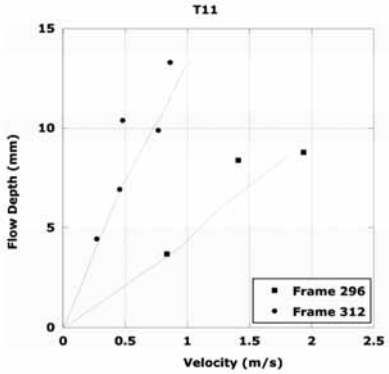

Fig. 7 - Velocity profile for T11.Frame 296 records the flow front, while 312 represents the falling limb, just after peak flow height

VELOCITY PROFILES

By tracking particles at various depths as the flow passed by the Perspex window, we attempted to reconstruct how velocity changed with depth as the flow front passed. One profile was taken at the flow front, while another was taken in the receding limb of the flow hydrograph, before the transition into the much finer, watery tail portion of the flow. Unfortunately, the epoxy used to seal the flume, and occasional residual material from previous tests, obscured the deepest 3 to 4 mm of flow, preventing a complete velocity profile to the base of the flume.

The flow front appears much faster and the velocity profile also less steep than that of the receding limb of the flow in all tests.

Examples are shown for T14 and T11 in Figures 6 and 7. The different velocity profile between the flow front and receding limb of the flow is due to two effects. The flow decelerates with time as is clear from the reducing discharge with time (see below). However, the very slow velocities shown for particles at depth after passage of the front is also caused by

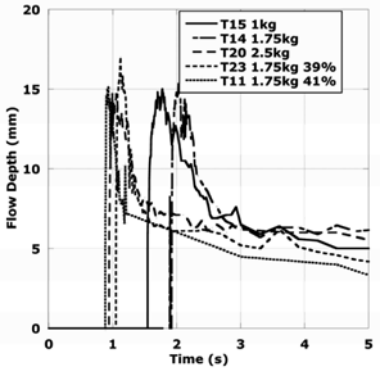

Fig. 8 - Flow depths versus time showing the passage of bouldery front and transition to finer, more watery tail

friction against the outer walls of the flume. In the high speed camera images, flow at the centre, which is not in contact with the side-walls, appears lighter than particles pressed against the window, due to the lighting set up. This enables the difference in surface velocity between edge and centre to be examined. At the very front of the flow, the flow margins were not in contact with the flume walls. Hence, this represents a velocity profile without the influence of friction from the walls of the flume. In the receding limb, the particles tracked are sliding against the window or wall.

FLOW DEPTH AND DISCHARGE

The flow depth of each test was recorded versus time and is shown in Figure 8. The most notable observation from these graphs is that maximum flow depth appeared to be approximately the same from test to test, irrespective of total flow mass and moisture content. This is likely to be a result of the boundary conditions as further discussed below.

Hydrographs were constructed for each test in order to explore how the discharge of each flow changed with time, as shown in Figure 9. Regression of flow depth against velocity gave a moderately linear relationship for each test. The resulting function was used to estimate an instantaneous surface velocity for each frame, based on the surface flow height observed in that frame.

Assuming the flow velocity decreases linearly with depth at any point during the flow [a reasonable first order approximation for a stony debris flow based on Takahashi (2007) and Figg. 6 and 7], the average flow velocity should be half of the observed surface velocity. A hydrograph was plotted frame by frame for each of the tests by multiplying this average velocity by the cross-sectional area. The resulting hydrographs were then integrated to calculate a total event volume.

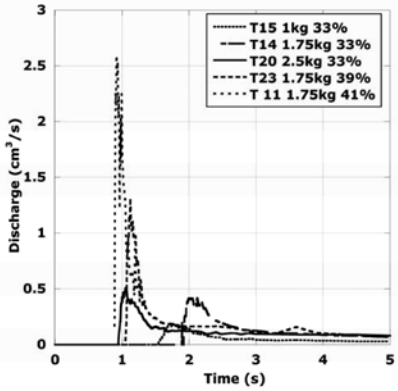

Fig. 9 - Hydrographs: calculated discharge versus time for each debris flow test

The total event volumes calculated from the hydrograph do show some differences between input and output measurements. The discrepancy between the amount of material entering the feeder tube and the amount of material recovered after the test was significant (on average 15%, and up to 25% in T11). This is mainly because not all of the material poured into the funnel reached the depositional surface. Some material remained in the feeder tube or was lost during the transition from the feeder tube and the head of the flume, especially in tests which were more fluid because material splashed off the flume surface in the abrupt transition between feeder tube and channel. In addition, a small amount of material may have been missed in collecting material from the drum surface.

Additionally, the hydrographs do not fully contain the extent of each flow because they are based on observations from the high speed camera, which was only able to record the first 18 seconds per test due to the memory constraints of the in-flight computer. Therefore, small amounts of flow continued after the last frame in each test, so that there was an unknown (albeit small) amount of deposition, which occurred after the camera had stopped recording that was not taken into account in the hydrograph.

Despite these limitations, comparing Figures 8 and 9 leads to some interesting qualitative observations of flow behaviour. That is, given that volume and moisture content in these tests had little effect on the maximum flow height, and hence the cross-sectional area, this suggests that the maximum cross-sectional area of flow was largely limited by the maximum flow rate available from the feeder tube. Given that the maximum cross-sectional area of each of the tests was similar, the velocity of the flow almost entirely controlled peak discharge. In turn, Figure 9 shows that a very small change in moisture content dramatically increases the flow discharge via an increase in flow velocity, independent of flow depth.

The stage hydrographs and velocity data show some similarity to field and large scale flume tests, as well as some differences. In a field-monitored debris flow in the Illgraben catchment in Switzerland, McArdell *et alii* (2007) report velocities of 1.4 m/s

for a gently sloping channel of 5 to 10º. Maximum flow depths were just over 1m. Video recordings indicated a strong conveyor belt-like circulation of particles and surface velocities were approximately twice the average velocity recorded in the camera imagery, closely resembling the behaviour in the centrifuge.

In large scale flume experiments, Denlinger & Iverson (2001) show stage hydrographs with peak flow heights of 0.2 m at 33 m from the head of the flume, reducing to 0.1 m at 67 m, compared to peak flow depths in our experiments of approximately 15mm (corresponding to 0.6 m at prototype scale) reducing to 5 mm (0.2 m at prototype scale) in the tail. While the shape of the peak response of the stage hydrograph is similar, the its trailing end differs significantly from the centrifuge tests. While the centrifuge flows display a thick, long running watery tail portion of the flow, the flow height in the large-scale flume tests quickly diminishes. This can be explained by the differing boundary conditions between tests. The large flume flows were triggered by a sudden release of a block of material, while material in the centrifuge tests was released more gradually via the feeder tube

The velocity in the USGS flume studies is markedly higher than in the centrifuge, at up to 10m/s (Denlinger & Iverson, 2001). This can be attributed to the much steeper, homogenous slope of the flume (31º) over its 95 m length. The centrifuge flows have much less time and length to accelerate and much less time for waveforms to accelerate, elongate, and extenuate when compared to the longer flume USGS flume (Denlinger & Iverson, 2001).

RUNOUT AND DEPOSITION

Point measurements of depth were used to construct contour plots of the deposition (Figg. 10 and 11). The morphology of deposition was strikingly similar in all tests. In contrast to many debris flows in the field and in large flume experiments (e.g. Denlinger & Iverson 2001), the width of lateral spread exceeded the runout of deposition. This is likely to be due to the rapid deceleration of the flow within the channel before opening to a horizontal deposition zone. In these experiments, unlike many other flume studies, the slope angle was continuously reducing from the head, at 36º, to the base, at near 0°. This means that the flow in all tests was moving relatively slowly upon reaching the deposition zone. In small

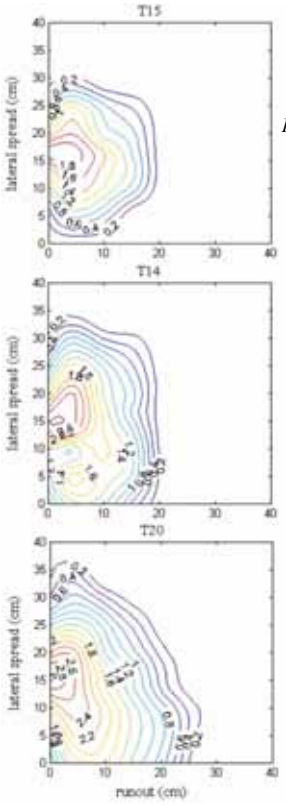

Fig. 10 - Deposition of T15 (1kg), T14 (1.75kg) and T20 (2.5kg) All flows run at 33% moisture content. Contour intervals are 0.2cm. Depth increases from cool to hot colors. The maximum contour is 3.0cm in T20

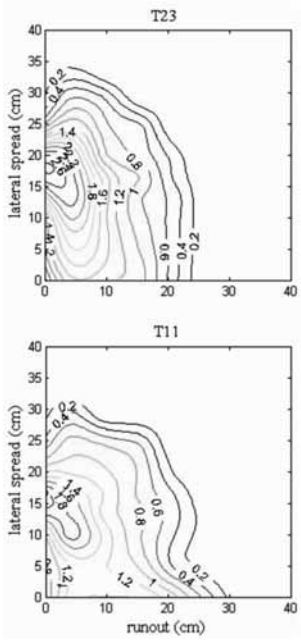

Fig. 11 - Deposition of T23 (1.75kg, 39% MC), and T11 (1.75kg, approximately 41% MC).

flume experiments, Bowman & Sanvitale (2009) found that deposition morphology (in terms of lateral spread and length) was largely a function of velocity at the exit point of the channel.

As expected, the depositional area increased with increased mass and moisture content. However, the effect of increased moisture content was much more important than an increase in mass. In fact, the overall deposition area between tests T20 and T23 was nearly identical, despite the fact that test T20 had more mass than T23. The higher mobility provided by the higher moisture content of T23 allowed it to spread thinner and farther than a flow of the same mass and lower moisture content (T14). This shows that pore pressures are key to reducing friction via a reduction in effective stress within a debris flow.

The contour plots, while useful for visualizing the morphology of deposition, were not well suited to analysing debris flow runout. Consequently, the centre of mass was calculated for each flow using the point depth measurements; this was used in the subsequent analysis of results.

Figures 12 through 14 show relationships between runout and the square of velocity, mass entering the flume and peak momentum of the flow, respectively.

Previous studies have found the flow runout to scale with velocity squared (Takahashi, 2007). While there is a clear linear relationship between the velocity squared and the runout for the flows at a moisture content of 33% (Figure 12), this relationship breaks down when flows at higher moisture contents are included. The flows with higher moisture contents run out far less than predicted, according to a linear squared velocity-runout relationship.

A better predictor of runout for the test flows conducted at 33% was the mass entering the flume (Figure 13). However, this was not entirely consistent. Flows undertaken at different moisture contents plot with different relationships.

Runout to the centre of mass of the flows increased with both moisture content and flow volume and showed a linear relationship (Figure 14) with in-

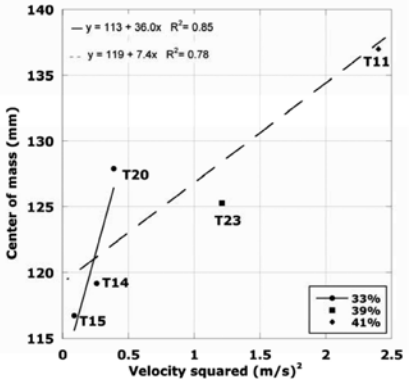

Fig. 12 - Location of centre of mass of deposition (measured from the flume exit) against velocity squared (measured at the high speed camera position). Trendlines for 33% moisture content flows (solid) and all flows (dashed) are shown. The test run at 41% moisture content is accurate to within ±1%, as discussed in the text

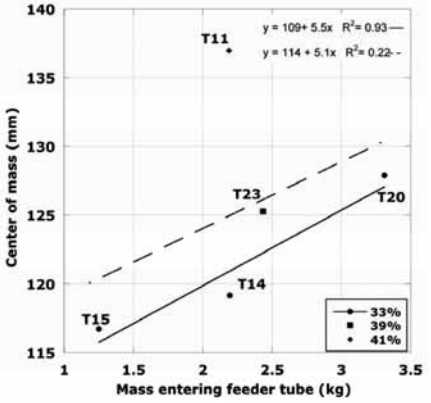

Fig 13 - Location of centre of mass of deposition (measured from the flume exit) against total mass of material entering the flume for each test. Trendlines are 33% moisture content (dashed) and all data (solid)

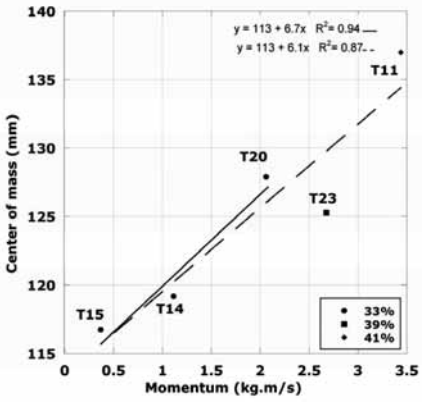

Fig. 14 - Location of center of mass of deposition (measured from the flume exit) against momentum of each flow (based on the velocity at the high speed camera position). Trendlines are 33% moisture content (solid) and all data (dashed)

creasing momentum at the high speed camera position, calculated as mass (in kg) multiplied by velocity (in m/s) at the high speed camera location.

Hence, it is hypothesised that because these flows displayed a low and homogenous velocity upon reaching the flume outlet, and because the peak cross-sectional area of the flow was limited by the feeder tube, lateral spread (which is determined by the total amount of material), largely governed the runout of these flows. Momentum, as it takes into account both the total mass and the velocity of the flow, shows a strong relationship with runout for all tests.

CONCLUSIONS

The five geotechnical centrifuge tests summarised in this paper demonstrate several important aspects of debris flow behaviour They also highlight some of the advantages and challenges of modelling debris flows in a geotechnical centrifuge.

Five debris flow tests were conducted in a geotechnical centrifuge at 40 g with variable volumes and moisture contents. Pore pressure and data derived from photographs taken with a high speed camera were used to construct plots of flow velocity with distance, flow height over time, velocity profiles with depth, and discharge over time, at one point in the flume.

Both an increase in volume and an increase in moisture content increased peak velocity during downslope movement. However, the effect of increased moisture content is much more pronounced than that of increased mass. The maximum cross-sectional area observed was limited by the flow diameter of the feeder tube. Consequently, flow velocity largely determined the peak discharge of each flow.

The large difference between the measured velocity profiles at the flow front, and during the recessional phase of the flow (but still in the coarse front), is explained by a general trend of decreasing velocity with time and friction against the flume walls.

An increase in moisture content increased the mobility of the flow in terms of inundated depositional area and runout. The runout of all flows can be related to the velocity, mass, and momentum. However, the momentum of the flow at the high speed camera position was the best predictor of runout in these experiments.

While aspects of centrifuge flow behaviour compare well with some field observations, the limited number of tests and experimental boundary conditions limit comparison with others. This paper provides an example of the kinds of data which can be generated from centrifuges tests, as well as some of the challenges and opportunities of using the technique. Based on these set of tests, a steeper flume configuration and larger diameter feeder tube, which would increase velocity, peak discharge, and the range of PSD tested, would be useful in the future.

Future work will compare the results from these flume tests with those predicted by analytical equations presented in the literature, as well as compare the effect of using a Newtonian vs. non-Newtonian pore fluid.

ACKNOWLEDGEMENTS

This research was made possible by a New Zealand Earthquake Commission Bi-annual grant, a University of Canterbury Doctoral Scholarship, and a New Zealand Postgraduate Study Abroad Award. Thanks go to the geotechnical group at ETH for their patience and generosity. A debt of gratitude is owed especially to Markus Iten, who was indispensable and irreplaceable before, during and after the experiments. The last two authors are members of the Competence Centre of Environmental Sustainability at ETHZ and contribute to a range of projects under this thematic partial funding for research into natural hazards (TRAMM, COGEAR, APUNCH).

REFERENCES

Bowman E.T., Laue, J., & Springman S. (2010) - *Experimental modelling of debris flow behaviour using a geotechnical centrifuge*. Canadian Geotechnical Journal, **47** (7)**:** 742-762.

Bowman E.T. & Sanvitale N. (2009) - *The role of particle size in the flow behaviour of saturated granular materials.* Paper read at 17th International Conference on Soil Mechanics and Geotechnical Engineering, at Alexandria.

D'Agostino V., Cesca M. & Marchi L. (2010) - *Field and laboratory investigations of runout distances of debris flows in the Dolomites (Eastern Italian Alps).* Geomorphology, **115** (3-4)**:** 294-304.

Denlinger R.P. & Iverson R.M. (2001) - Flow of variably fluidized granular masses across three-dimensional terrain: 2. Numerical predictions and experimental tests. J. Geophys. Res, **106:** 553-566.

Fannin R.J. & Wise M.P. (2001) - *An empirical-statistical model for debris flow travel distance*. Canadian Geotechnical Journal,

38 (5)**:** 982-994.

Hungr O., Morgan G., & Kellerhals P. (1984) - *Quantitative Analysis of Debris Torrent Hazards for Design of Remedial Measures*. Canadian Geotechnical Journal, **21** (4)**:** 663–677.

King J. (1996) - *Tsing Shan debris flow. In Special Project Report SPR 6/96. Geotechnical Engineering.* Office, Hong Kong Government, Hong Kong. p. 133.

McArdell B.W., Bartelt P. & Kowalski J. (2007) - *Field observations of basal forces and fluid pore pressure in a debris flow.* Geophysical Research Letters, **34** (7)**:** 74-76.

Pierson T. (1980) - *Erosion and deposition by debris flows at Mt. Thomas, North Canterbury, New Zealand*. Earth Surface Processes, **5:** 227-247.

Rickenmann D. (1999) - *Empirical Relationships for Debris Flow*s. Natural Hazards, **19** (1)**:** 47-77.

Springman S., Laue J., Boyle R., White J, & Zweidler A. (2001) - *The ETH Zurich Geotechnical Drum Centrifuge*. International Journal of Physical Modelling in Geotechnics, **1** (1)**:** 59-70.

Steedman R.S. & Zeng X. (1995) - Dynamics. In: Taylor R.N. (1995, ed.) - *Geotechnical Centrifuge Technology*. Blackie Academic & Professional, Glasgow.

Takahashi T. (2007) - *Debris flow: mechanics, prediction and countermeasures*. Routledge. Taylor & Francis Group, London.

